					Median intensities (cell types and groups)									
	SeqID	SeqName		Earray_Refseq	H23	H522	ScaBER	T24	H358	H441	HT1376	non-permissive	permissive	median distance
1	652903	TMEM45B	*2,3	NM_138788	1.095	1.128	5.065	3.045	11.872	15.370	9.485	1.622	11.872	10.250
2	655324	CLDN7	*1	NM_001307	4.153	5.007	12.941	5.357	13.441	14.044	14.444	5.027	14.044	9.017
3	672299	TMEM125	*2,3	NM_144626	6.073	3.920	9.911	5.225	14.186	14.759	14.032	5.295	14.186	8.891
4	660062	GPR110	*2,3	NM_153840	1.037	1.175	11.683	10.577	14.591	15.663	11.851	5.789	14.591	8.802
5	642093	CLDN4	*1	NM_001305	2.901	3.131	9.426	4.223	12.603	12.064	12.629	3.827	12.497	8.670
6	654402	ST14	*2	NM_021978	4.874	5.673	11.969	5.639	13.405	13.913	13.096	5.656	13.473	7.818
7	656701	EPHA1	*2	NM_005232	1.624	1.386	8.080	1.490	9.596	9.489	8.769	1.703	9.428	7.725
8	676384	MCTP2	*2,3	NM_018349	1.362	1.045	7.288	1.130	8.753	9.536	8.827	1.179	8.833	7.655
9	643771	PVRL4	*2	NM_030916	1.705	0.998	6.312	1.129	8.875	8.781	11.287	1.666	8.875	7.209
10	648785	CSF2RA	*2	NM_172247	5.185	2.971	2.884	1.155	7.504	10.486	10.066	2.907	10.066	7.159
11	660004	ENPP5		NM_021572	3.523	0.917	6.791	0.890	8.832	10.028	7.068	1.794	8.832	7.038
12	673718	TREM1	*2	NM_018643	2.075	0.971	1.027	1.056	7.939	11.902	5.470	1.024	7.939	6.916
13	681511	GPA33	*2	NM_005814	1.717	3.327	1.365	1.022	8.573	9.502	6.949	1.683	8.573	6.890
14	658566	TNFRSF10C		NM_003841	3.853	1.058	1.038	3.879	9.750	8.076	6.520	1.394	8.076	6.682
15	656363	SCNN1A	*2,3	NM_001038	4.607	0.990	4.451	6.514	11.126	12.077	10.680	4.529	11.126	6.597
16	652933	PTAFR		NM_000952	4.060	4.446	8.679	4.075	11.329	10.801	10.283	4.337	10.790	6.453
17	664396	ANKRD22		NM_144590	7.644	0.898	8.654	0.932	11.214	9.656	11.249	4.854	11.214	6.359
18	662347	SLCO4C1		NM_180991	5.367	1.053	0.907	1.183	6.248	7.485	7.534	1.059	7.158	6.100
19	671227	MUC15		NM_145650	0.920	4.474	0.933	0.983	7.051	6.507	9.769	0.964	7.051	6.086
20	671510	TNFSF15		NM_005118	1.554	1.033	3.603	1.074	7.356	5.272	6.587	1.105	6.587	5.482
21	668056	KRTCAP3	*2,3	NM_173853	6.384	5.598	10.608	4.881	12.060	10.774	11.293	5.880	11.331	5.451
22	651936	MUC1		NM_002456	9.906	8.317	10.528	7.313	11.729	14.816	14.202	9.122	14.202	5.080
23	666420	EGF		NM_001963	1.191	1.199	3.756	2.247	8.275	6.830	4.886	1.825	6.830	5.006
24	678827	TMC4	*2,3	NM_144686	5.842	5.809	8.383	5.908	10.739	10.988	8.476	6.112	10.667	4.555
25	675238	FCGR2A	*2	NM_021642	3.993	4.174	3.343	2.866	9.051	8.305	4.866	3.777	8.305	4.528
26	668630	MUC16		NM_024690	5.622	2.335	5.644	2.573	8.916	6.917	10.286	4.427	8.916	4.489
27	644414	ERBB3	*1	NM_001982	7.304	5.074	9.156	4.170	10.475	11.567	10.743	6.483	10.839	4.355
28	672447	C19orf46	*2	NM_001039876	8.344	8.348	6.889	6.077	12.767	11.777	11.766	7.547	11.815	4.268
29	677376	C1orf210	*2,3	NM_182517	2.976	3.230	5.837	1.116	6.831	7.545	9.152	3.286	7.545	4.259
30	678029	GPR37		NM_005302	9.101	3.104	6.321	3.754	9.241	10.674	9.563	5.316	9.563	4.247
31	662729	ZPLD1	*2	NM_175056	0.894	0.895	0.866	0.884	4.821	6.345	5.085	0.882	5.085	4.204
32	679847	MAL2	*2	NM_052886	10.573	2.899	13.398	11.964	15.452	15.516	14.554	11.252	15.428	4.175
33	664418	C6orf25	*2	NM_138272	2.214	2.313	1.936	0.989	6.155	5.350	7.779	2.075	6.155	4.080
34	652336	ADAM28		NM_021777	1.355	0.993	2.463	1.147	5.179	6.287	2.597	1.182	5.179	3.997
35	652634	SPINT1		NM_181642	7.067	5.027	11.114	9.481	12.302	12.091	11.129	8.143	12.091	3.948
36	681183	PKD1L2		NM_001076780	0.983	2.140	2.438	1.081	5.256	3.326	5.370	1.223	5.141	3.919
37	641358	TMC5	*2,3	NM_024780	7.083	7.306	7.410	1.146	10.512	13.613	10.920	7.072	10.920	3.848
38	657781	MPZL3	*2,3	NM_198275.1	6.836	7.802	8.771	9.361	12.142	11.624	11.933	8.337	11.933	3.597
39	641507	AREG		NM_001657	11.929	13.596	15.424	11.130	16.567	16.106	15.718	12.474	16.060	3.586
40	662097	FAM62C		NM_031913	4.036	1.137	2.060	1.102	4.512	5.184	6.696	1.599	5.184	3.585
41	660608	MST1R	*2,3	NM_002447	6.004	4.432	10.582	10.604	11.571	11.594	12.267	8.289	11.866	3.577
50	659480	CLDN3	*1	NM_001306	9.726	9.699	5.843	6.410	12.876	11.192	10.711	8.136	11.192	3.056
51	651178	ATP1B1	*1	NM_001677	11.681	10.629	14.082	13.155	15.771	15.611	15.095	12.354	15.349	2.995
53	680370	PLLP	*2,3	NM_015993	6.510	5.257	5.667	5.258	7.732	8.125	9.363	5.590	8.423	2.833
54	681571	EMP2	*2,3	NM_001424	9.136	10.534	10.430	9.606	12.021	12.696	14.497	9.887	12.696	2.809
62	644613	KCNN4	*2,3	NM_002250	11.308	7.861	11.383	9.344	13.162	12.115	12.847	10.315	12.847	2.532
79	649702	CYB561	*2,3	NM_001017916	9.786	8.208	11.592	11.139	12.427	12.580	11.995	10.455	12.427	1.971
99	677059	ZDHHC21	*2,3	NM_178566	7.959	8.605	7.835	8.985	9.772	9.537	9.445	8.170	9.589	1.420
206	665985	C3AR1	*2	NM_004054	7.223	7.381	7.207	7.374	7.668	7.527	7.877	7.298	7.668	0.370

Supplementary Table 1. Surface associated proteins upregulated in MV permissive vs. non-permissive epithelial cell lines.

Footnotes: 1, tested in screen 1; 2, tested in screen 2; 3: significantly up-regulated mRNAs in both screens. Further proteins tested in screen 1 not in the table: P2RY2 (NM_002564), EFNB2 (NM_004093), CDH1 (NM_004360), ITGA3 (NM_002204), MYO1D (NM_015194), SLC2A1 (NM_006516), ITGB4 (NM_000213), PVRL3 (NM_015480), TRIP6 (NM_003302), CLDN12 (NM_012129), MET (NM_000245), MUC20 (NM_001098516), P2RY6 (NM_004154), SLAMF7 (NM_021181), AQP4 (NM_001650), SDC2 (NM_002998). Values represent the log2 values of quantile normalized mRNA expression intensities.

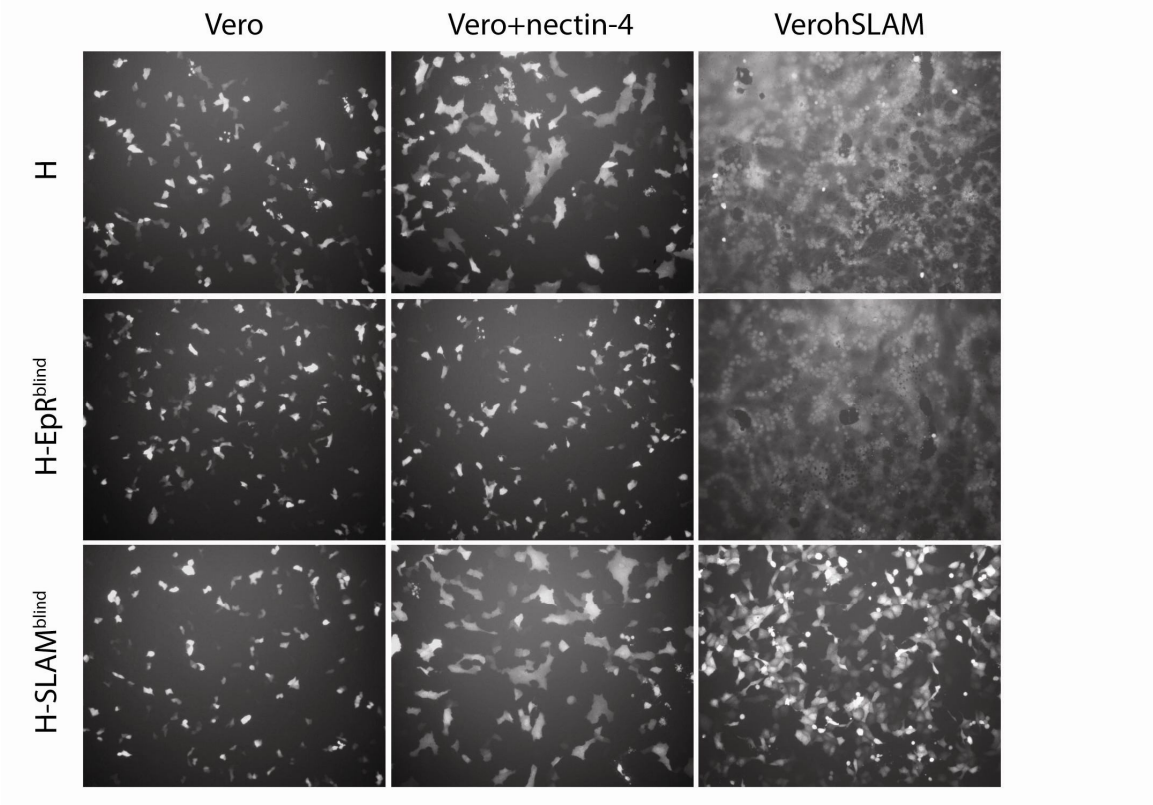

Supplementary Fig. 1. Expression of nectin-4 confers MV glycoprotein-dependent membrane fusion.
To assess nectin-4 function we transiently co-expressed it with both MV glycoproteins F and H, and GFP to visualize transfected cells. H is the receptor-binding protein, while F fuses the donor and acceptor membranes. Vero cells not expressing a receptor were mock-transfected (first column), or transfected with a nectin-4 expression plasmid (second column). In addition, plasmids expressing the three variants of the H protein indicated on the left (H-EpR^{blind}, H, and H-SLAM^{blind}), were co-transfected with a F-expressing plasmid, and a GFP-expressing plasmid that allowed visualizing the transfected cells. The "receptor-blind" proteins have mutations disallowing entry selectively through one receptor[13].The plasmids expressing the different H proteins were also co-transfected with a GFP-expressing plasmid in VerohSLAM cells expressing the SLAM receptor (third column). While co-expression of standard H and F proteins elicited fusion of cells expressing either SLAM or nectin-4 (first row, second to third panels), the selectively EpR-blind H protein sustained fusion only of SLAM-expressing cells (second row, third panel). Conversely, the SLAM-blind H protein sustained fusion only of cells expressing nectin-4 (third row, second panel). Since nectin-4 is functionally equivalent to the EpR, we renamed MV-EpR^{blind} as MV-nectin4^{blind}.

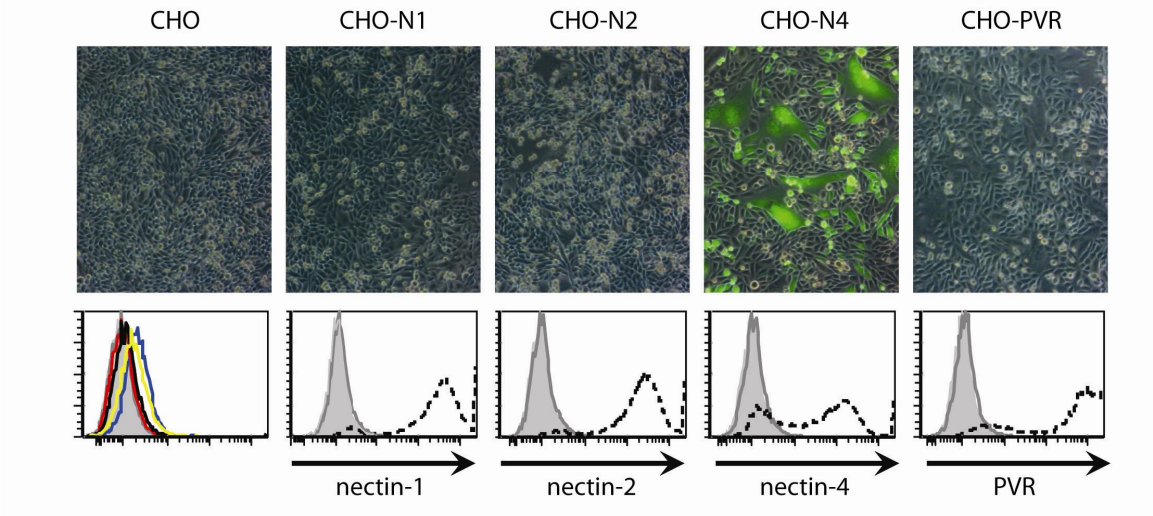

Supplementary Fig. 2. Nectin-4, but not other human nectins or the related poliovirus receptor (PVR), has MV receptor function.
Top row: MV-GFP infection of Chinese hamster ovary (CHO) cells (left panel), or CHO-derived stable cell lines expressing the four members of the PVRL/nectin protein family indicated on the top (second to fifth panels). CHO-N1, -N2 and -N4: CHO cells expressing human nectin-1, -2, or -4, respectively. CHO-PVR: cells expressing the poliovirus receptor (PCR), the original member of this protein family. Nectin-3 was tested in our original screen with the other 21 receptor candidates, but did not sustain MV entry (Supplementary Table 1, footnote). Only cells expressing nectin-4 formed syncytia that emitted green fluorescence after MV-GFP infection. Bottom row: expression of nectin family proteins was confirmed by FACS analysis. All panels: grey shading, unstained controls; grey solid line, isotype controls; black dashed line, staining against relevant nectins. First panel: blue/red/black/yellow solid lines, anti-nectin1/2/4/PVR staining, respectively.

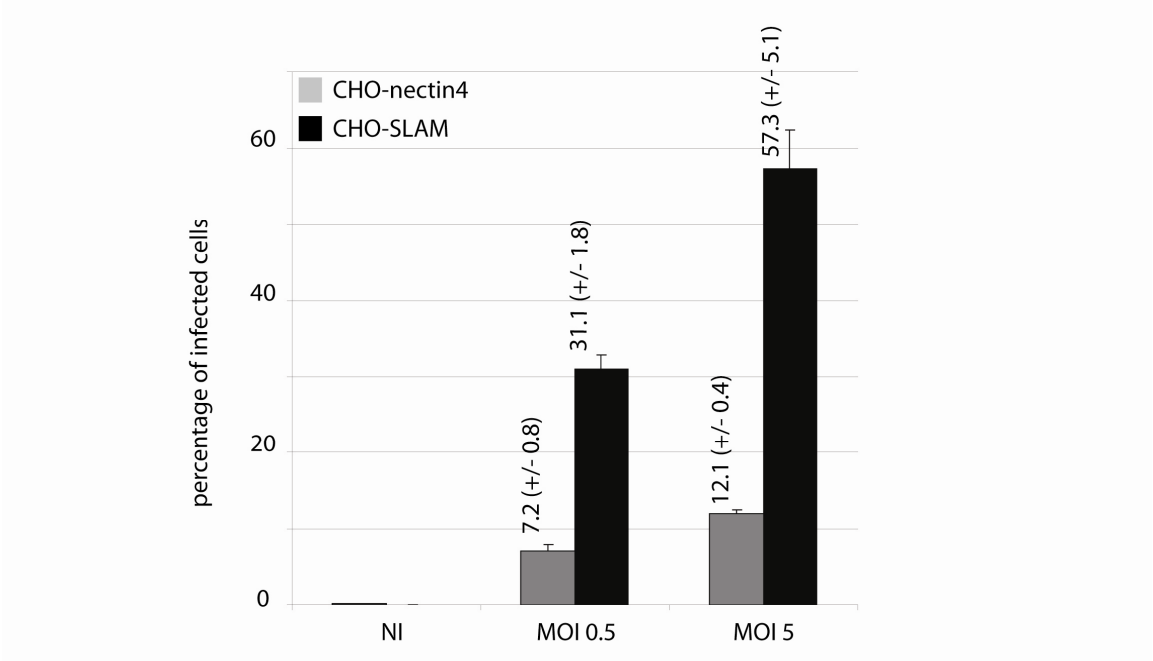

Supplementary Fig. 3. MV infects and replicates more efficiently in SLAM-expressing cells than in nectin4-expressing cells.
To assess the MV infectivity depending on the receptor, we infected CHO-nectin4 or CHO-SLAM stable cell lines with MV at a MOI of 0.5 or 5 with a MV-GFP virus. At 4 hrs post infection, the medium was replaced by medium containing the fusion-inhibiting peptide Z-d-Phe-l-Phe-Gly-OH (FIP). At 48 hrs post infection, the cells were harvested and stained for the surface expression of nectin-4 or SLAM. We then determined the percentage of infected cells (expressing GFP) in the population of cells expressing the receptor by FACS analysis. The graphs represent the means and standard deviations of experiments performed in duplicates (NI) or triplicates (MOI 0.5 and MOI 5).

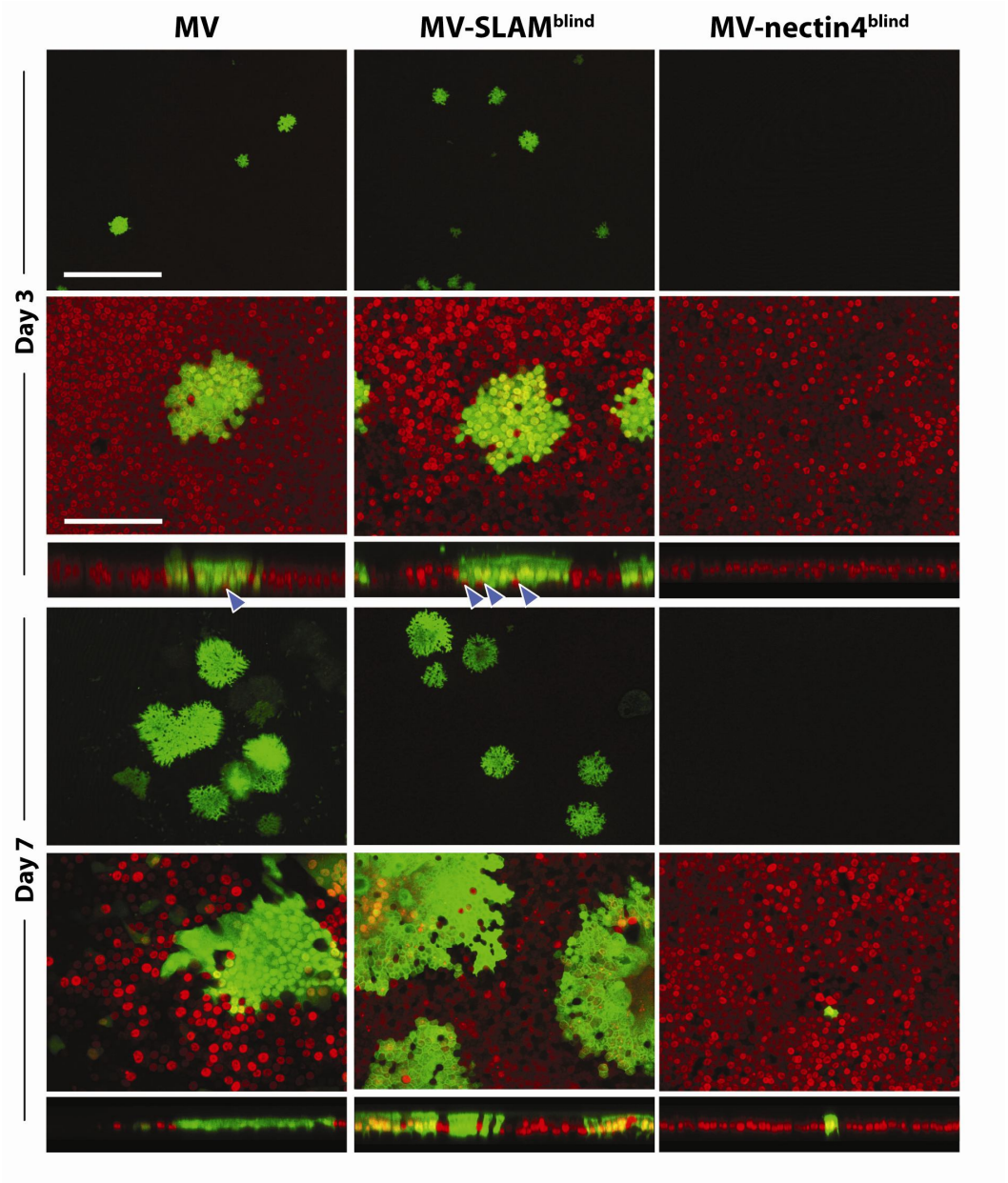

Supplementary Fig. 4. MV not recognizing nectin-4 does not spread in human airway epithelia.
Confocal images were taken 3 days (panels in top half) or 7 days (panels in bottom half) after basolateral virus inoculation at a MOI of 0.1. In both analyses the top panel is a low power image (scale bar = 500 microns), the center panel is a high power image, and the bottom panel is a vertical section of the center panel (scale bar = 100 microns). MV and MV-SLAM^{blind} infections were cell-type selective: only ciliated columnar cells spanning the epithelium and with the ACC were infected, while basal cells located at the base of the epithelium were spared (left and center columns, days 3 and 7; marked with arrowheads in day 3 panel). Infections of all viruses often regressed after 1-2 weeks (data not shown), possibly due to innate immune functions of these primary cells. Confocal images were captured with a Bio-Rad Radiance 2100 multiphoton confocal microscope. Cell nuclei were counterstained with TO-PRO-3 (red).

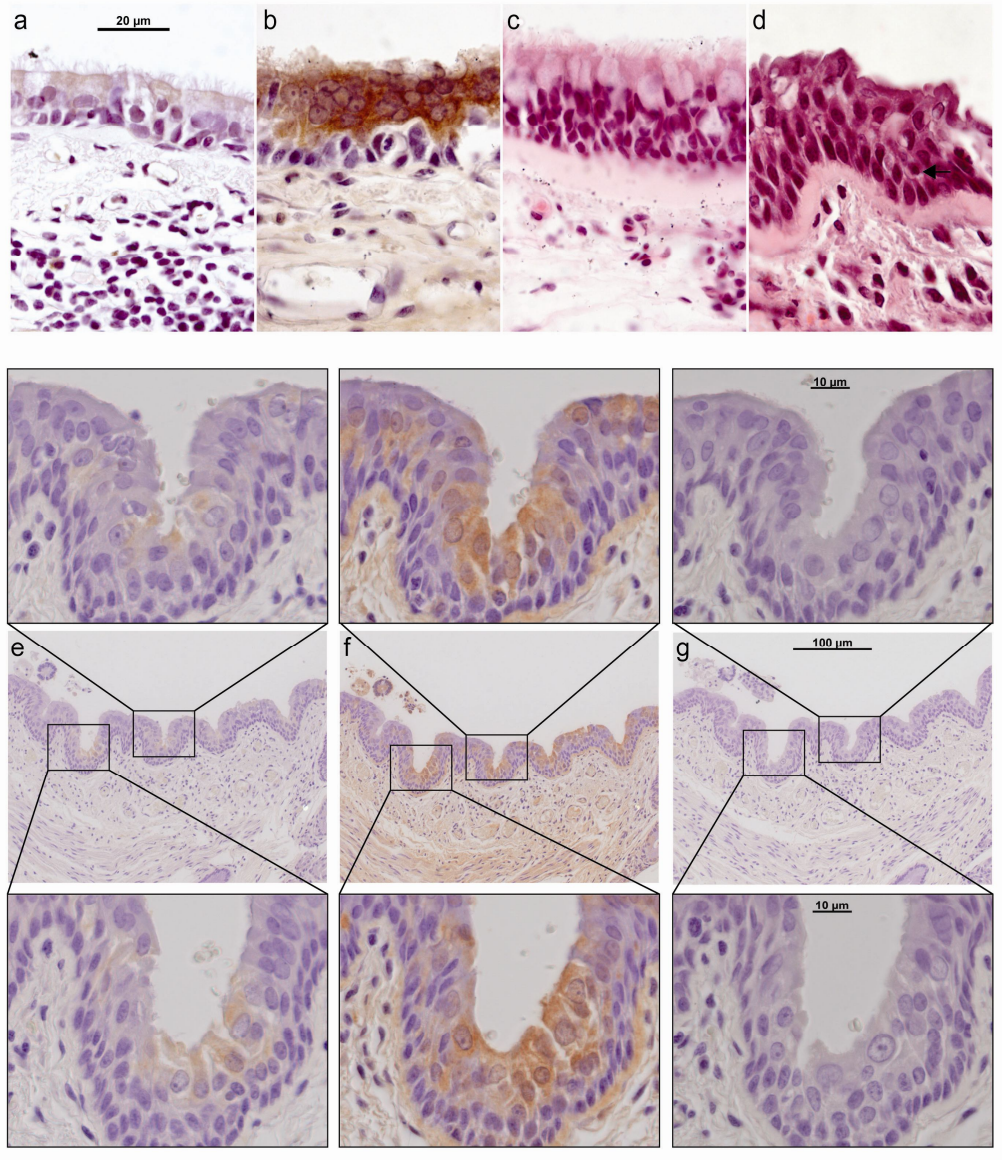

Supplementary Fig. 5. Multifocal infection of nectin-4 expressing cells in monkey tracheal epithelium 12 days after inoculation with MV.
a and b, paraffin sections stained with a non-specific antibody (a) or an antibody against the viral nucleocapsid (b) and counterstained with eosin as described in the Online Methods section at 100x magnification. c and d, hematoxylin- stained paraffin sections of trachea from control (c) and infected (d) animals at 100x magnification. Morphological changes were noted, including focal destruction of the multilayer epithelia with loss of goblet cells and cilia, occasional possible inclusion bodies (arrow in d), and areas of epithelial hyperplasia. e-g, paraffin sections stained with an antibody against the viral nucleocapsid (e), a nectin-4 antibody (f), or a non-specific antibody (g) at 20x magnification. The areas indicated by boxes are also shown at 100x magnification. Multifocal viral infection was monitored in nectin-4 expressing cells (insets in e).

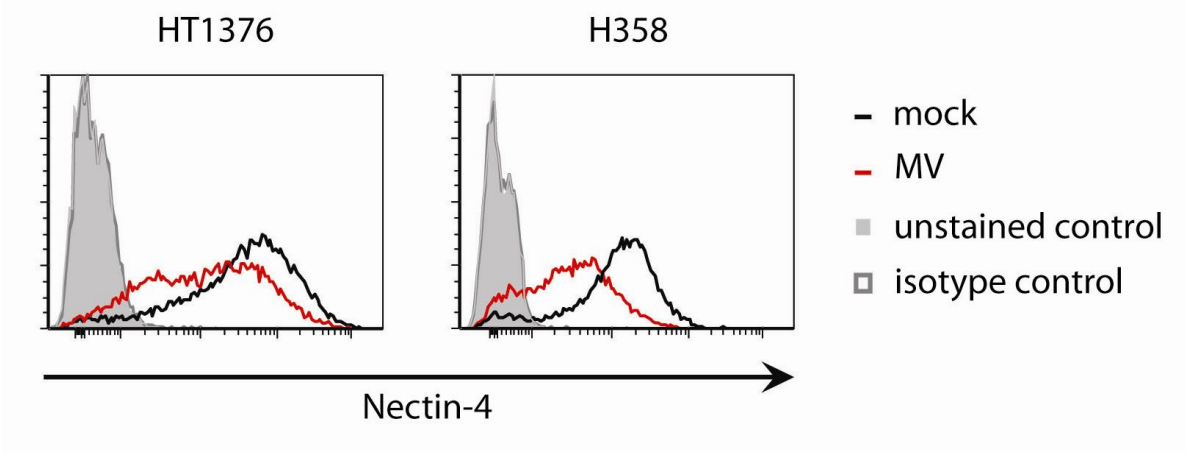

Supplementary Fig. 6. Nectin-4 is downregulated after MV infection.
To assess downregulation of nectin-4 after MV infection, lung (H358) and bladder (HT1376) epithelial cell lines expressing nectin-4 were infected with MV at a MOI of 1. Nectin-4 expression levels of mock (black solid line) and MV (red solid line) infected cells were assessed 48 hrs after infection by FACS analysis. For this purpose, cells were detached, stained for nectin-4 expression as described in online methods, and analyzed on an LSRII-SORP analyzer using Diva software (BD Biosciences). Dark grey lines: isotype controls; light grey shadings: unstained controls. Vertical axis: cell number. Horizontal axis: level of nectin-4 expression.

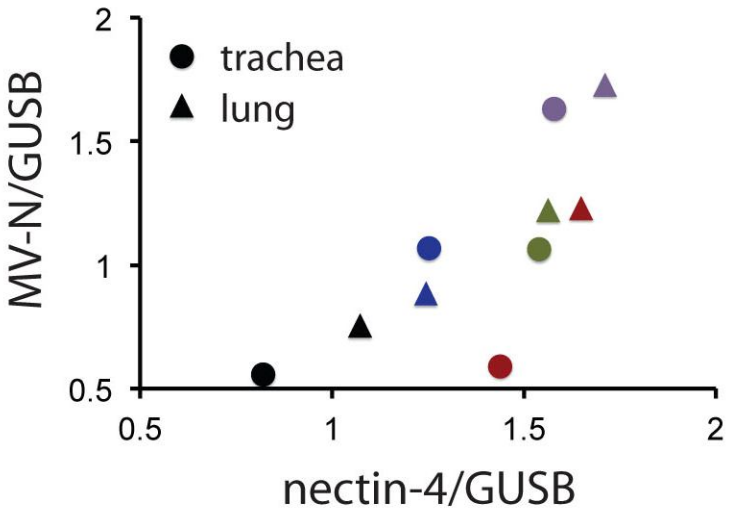

Supplementary Fig. 7. MV infection correlates with nectin-4 expression levels in airway tissue of cynomolgus macaques.
Real time PCR was used to quantify MV nucleoprotein (N), nectin-4, and β-glucuronidase (GUSB) mRNA levels in trachea and lung tissues isolated from infected cynomolgus macaques. X-axis: MV N/GUSB Ct ratio of each sample. Y-axis: nectin-4/GUSB Ct ratios. Different colors indicate different individuals. The correlation coefficient r was 0.77 (high). We suggest this correlation is due to the fact that a threshold level of nectin-4 expression is required for productive infection. Frozen trachea, lung, and bladder samples harvested from one control non-infected and five infected cynomolgus macaques on day 12 after infection were weighed, homogenized in RLT buffer (QIAgen) containing 1% β-mercaptoethanol, and total cellular RNA was extracted (RNeasy Mini, Qiagen). The QuantiTect SYBR Green RT-PCR kit (QIAgen) was used to quantify MV N and nectin-4 mRNA levels compared to the housekeeping gene β-glucuronidase in different tissues following the manufacturer's protocol using a RotorGene RG-3000A thermocycler (Corbett). Primers for MV N and nectin-4 will be available on request, and commercial primers (SA Biosciences/QIAgen) were used to amplify β-glucuronidase. Melting curve analysis and quantification were performed using the RotorGene 6.0 software package (Corbett).

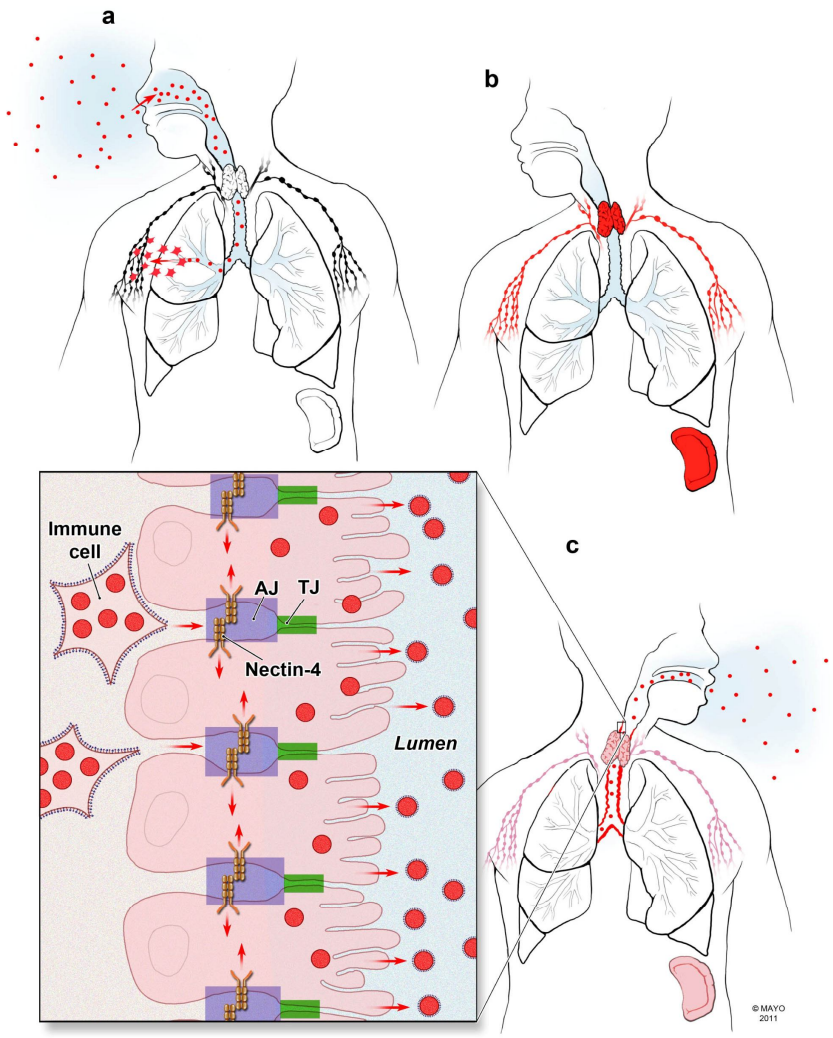

Supplementary Fig. 8. Model of the MV infectious cycle.
In the lymphatic phase of infection (a and b) SLAM is used as receptor; in the epithelial phase (c and inset) nectin-4 is used. Infectious viral particles are shown as red spheres; viral glycoproteins are drawn as small spikes on the spheres in the inset close-up. Infected cells and organs are shown in red at the peak of infection in one organ, or in pink after the peak. a, MV enters the airways and infects macrophages and dendritic cells, which ferry the infection to the local lymph nodes. b, MV infects the local lymph nodes and the infection spreads rapidly to the primary lymphatic organs thymus and spleen (shown in red). c, infection spreads to the epithelium. Inset: MV enters the epithelium of the airways carried from an infected immune cell that expresses the viral glycoproteins on its plasma membrane. The viral H protein binds to nectin-4 (yellow) in the adherens junction (AJ, blue rectangle), which is located basolateral to the tight junction (TJ, green rectangle). Infection spreads laterally via tight junctions (red arrows). Epithelial cells express viral glycoproteins in their membranes (not shown for simplicity). Progeny viral particles are released in the trachea (epithelium shown in red) and expulsed by coughing and sneezing.